Biointerface Research in Applied Chemistry
Open-Access Journal (ISSN: 2069-5837)

Article
Volume 14, Issue 4, 2024, 90
https://doi.org/10.33263/BRIAC144.090

Studies on Optical Band Gap and Optical Conductivity of *Ex-situ* Fabricated rGO:V_2O_5 Composites

Aanchal Sharma [1], Pawan Sharma [1], Nandan Singh Karki [2], Manisha Bisht [2], Goverdhan Singh [1], Anil Kumar [1], and Harish Mudila [1,*]

[1] Department of Chemistry; Lovely Professional University, Punjab-144411, India
[2] Department of Chemistry, L.S.M.G.P.G.C., Pithoragarh-262502, Uttarakhand-262501 India
* Correspondence: harismudila@gmail.com;

Scopus Author ID 56372911400
Received: 22.11.2023; Accepted: 20.12.2023; Published: 20.07.2024

Abstract: In this present study, Graphene oxide (GO) is synthesized by modified Hummer's method. The GO formed is further used to prepare V_2O_5 embellished reduced graphene oxide (rGO) composites (rGO: V_2O_5) in varying ratios via an in-situ process. UV-Vis spectroscopy was employed to study optical properties such as band gap and optical conductivity of the composites and individual species. rGO synthesized was studied to have a narrow band gap of 1.93 eV, which was much lower than the metal oxide used. Thus, rGO enticing material is to be used to modify the band gap of the prepared composites, thus lowering the optical band gap to 1.32 eV for rGO: V_2O_5 (2:1) and enhancing the optical conductivity to 5.34×10^{10} $S.cm^{-1}$. Characterization of the compound is done using various analytical techniques, including FTIR, SEM, XRD, and TGA. All these studies designate the successful fabrication of the required composites with specific properties. Thus, it is concluded from the study that rGO:V_2O_5 in 2:1 can be used as a potent material in optoelectronic applications.

Keywords: Clean and affordable energy, optical conductivity, optical band gap, reduced graphene oxide, V_2O_5.

1. Introduction

In recent years, the study of the optical properties of material has been an interesting area of research due to the increasing demand for advanced materials with unique electronic and optical properties [1]. In current studies, rGO and V_2O_5 synthesize a hybrid material with better optical activity than the individual material.

V_2O_5 was chosen for the research due to its remarkable properties, such as good adsorption in visible regions, electrical conductivity, and great electrochemical performance. Along with this, V_2O_5 is an easily available and efficacious material [2-4]. rGO has been used due to its ability to act as a supporting material for charge transport. rGO consists of many important properties, such as electrical conductivity, large surface area, and good optical properties [5-8].

Various studies have been done to investigate the optical properties of rGO: V_2O_5 composites that are obtained by the *ex-situ* fabrication method. One of the important optical properties of these materials is the optical band gap, which measures the energy required to excite the electrons from the valance band to the conduction band. This is a significant property

for designing and developing devices like solar cells, photodetectors, and light-emitting diodes [9-10].

Optical conductivity is a property of the material that determines its ability to conduct light. Knowing the optical conductivity of rGO : V_2O_5 composites can optimize their optical performance for numerous applications. Thus, it is an important area to research as it can potentially contribute to developing advanced optical and electronic devices [11-13]. In this research work, rGO is composited with V_2O_5 in different ratios to study the synergetic impact of V_2O_5 and rGO with each other. The exciting results make these composites a promising contender for optoelectronic applications.

2. Materials and Methods

2.1. Materials.

Graphite, Conc. Sulphuric acid (H_2SO_4), Potassium permanganate ($KMnO_4$), Ascorbic acid, Hydrochloric acid (HCl), 30% Hydrogen peroxide (H_2O_2), and V_2O_5 are purchased from Loba Chemie Pvt. Ltd.

2.2. Synthesis of GO from graphite.

GO is synthesized from graphite by using Modified Hummer's method. 5g of Graphite powder is taken in a 500 ml beaker, to which 75 ml of concentrated H_2SO_4 is added. 15 g of $KMnO_4$ is added very slowly to the reaction. The material was stirred for 2 hours at a maintained temperature of 5°C. Afterward, the temperature increased to 35°C, and the material was kept vigorously stirred for 30 minutes. 200 ml deionized water is added to the above solution, which generates a temperature rise from 35-98°C owing to the heat of hydration. Stirring is continued for the next 45 minutes at the temperature mentioned above. 140 ml deionized water and 20 ml H_2O_2 (30 wt. %) is then added, which results in the generation of yellow-brown precipitates of GO. Further, on vacuum filtration, the precipitates are separated and washed with 5% aqueous HCl. The obtained filtrate was dried for 24 hours at 60°C in a vacuum oven [14-15].

2.3. Synthesis of rGO by ascorbic acid.

GO is transformed to rGO with the help of ascorbic acid. 1g of GO prepared earlier is dispersed in 400 ml of water. 10 g of ascorbic acid is added to the solution and is allowed to stir for 120 minutes at 60°C. The product is obtained as a thick black slurry and is collected with the help of centrifugation. 10-20 ml H_2O_2 (30 wt. %) was added to the reaction mixture, and it was stirred for 30 minutes at 60°C to remove excess ascorbic acid. A black-colored product is obtained and washed with ethanol and water 3-4 times. The product is collected with the help of centrifugation and dried at 120°C for 24 hours [16-17].

2.4. Preparation of composite ratios.

Composite of rGO and metal oxide V_2O_5 are prepared in varying ratios of 1:1, 1:2, and 2:1 using the solvothermal method. rGO is prepared by reducing GO with the help of ascorbic acid. V_2O_5 is added to the rGO formed, and stirring is continued for 1 hour at 60°C (Scheme 1). The product is sonicated for 30 minutes at room temperature for better insertion of V_2O_5 in

the rGO layers. The product is obtained by centrifugation followed by decantation. The ratios are dried at 60°C and ground to powder form [18].

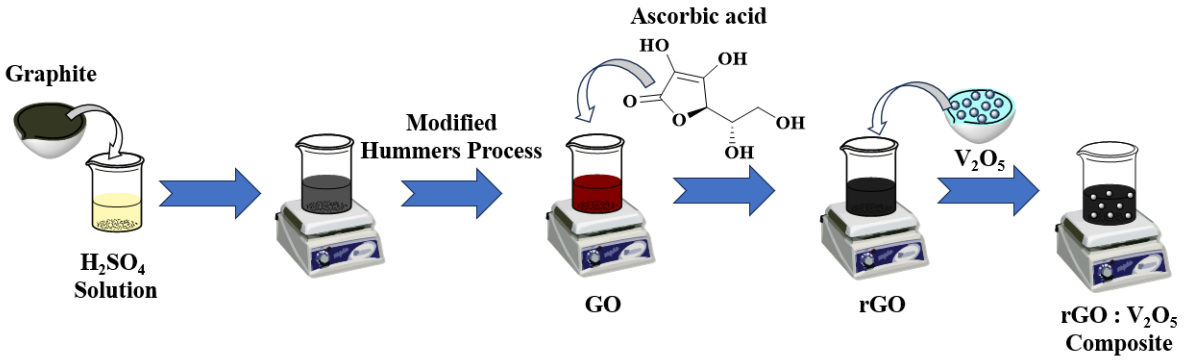

Scheme 1. Diagrammatic representation of the preparation of rGO : V_2O_5 composite.

3. Results and Discussion

3.1. UV-Vis spectroscopy.

UV-Vis spectroscopy is used to study the optical properties of the compounds. Characterization of compounds is done by using ethanol as a solvent. The instrument used for the analysis is a Shimadzu UV-1900i spectrometer with a wavelength range of 200-800 nm. According to the data collected with the help of UV-Vis spectroscopy, the peaks observed at 245 nm in GO are slightly shifted to 279.78 nm in rGO. This peak shift shows the rearrangement of graphene sheets after the reduction process [19]. The peaks observed in GO at 245 nm and 310 nm are of π to π* and n to π* transitions due to the presence of C=C bonds and C=O bonds, respectively. As GO is reduced to rGO, a red shift is observed [20-21] (Figure 1).

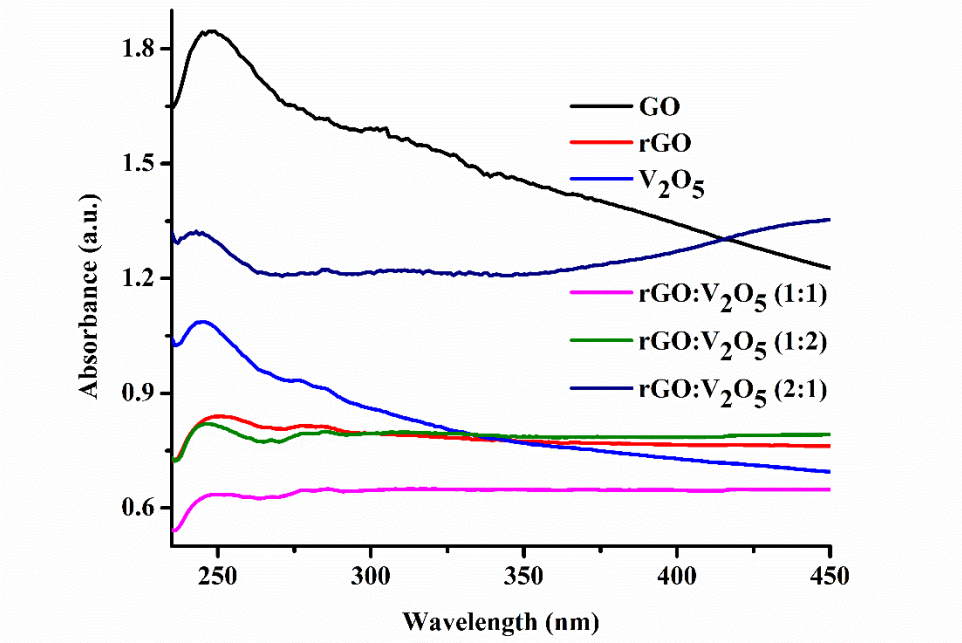

Figure 1. UV-Vis absorption spectra of all individual and composite materials.

Band gap is an intrinsic property of an optically conductive material; the band gap is observed for different ratios of the rGO:V_2O_5 composites, V_2O_5, and rGO with the help of UV-Vis spectroscopy. For rGO, the observed band gap lies near 1.93 eV, while for V_2O_5, the band

gap lies around 2.82eV (Figure 2a); the results follow the reported studies [22-23]. When the band gap of composites was studied, a decrease in the band gap of metal oxide V_2O_5 was seen for 1:1 and 2:1 samples. It is expected as such due to the introduction of defects in the composites leading to an increase in charge carrier density and mobility. Whereas in 1:2 sample, an increase in the band gap is observed. It may be due to the higher band gap of transition metal oxide V_2O_5.

Optical conductivity is calculated for all the samples. It has been observed that optical conductivity for V_2O_5 and rGO is 2.07×10^{10} and 3.55×10^{10} $S.cm^{-1}$, respectively (Figure 2 b). The optical conductivity for the rGO:V_2O_5 composites that were studied has been observed in various ratios of composites (Table 1). The formulas used for calculating optical conductivity are as follows:

Transmittance (T):

$$T = exp\ (-2.303\ A) \ldots\ldots\ldots (1)$$

Reflectance (R):

$$T = (1-R)^2 exp\ (-A) \ldots\ldots\ldots (2)$$

Reflectance has been used to calculate the reflective index (n) with the help of the following formula:

$$n = \left(\frac{4R}{(R-1)^2} - K^2\right)^{1/2} - \frac{(R+1)}{(R-1)} \ldots\ldots\ldots (3)$$

Extinction coefficient (K):

$$k = \frac{\lambda\alpha}{4\pi} \ldots\ldots\ldots (4)$$

Optical conductivity(σ):

$$\sigma = \frac{\alpha n c}{4\pi} \ldots\ldots\ldots (5)\ [24]$$

Table 1. Observed band gap and optical conductivity of rGO, V_2O_5, and synthesized composites.

Compound	Observed band gap (eV)	Optical conductivity×10^{10} ($S.cm^{-1}$)
rGO	1.97	3.55
V_2O_5	2.82	2.07
rGO : V_2O_5 (1:1)	2.34	2.16
rGO : V_2O_5 (1:2)	3.21	1.30
rGO : V_2O_5 (2:1)	1.32	5.34

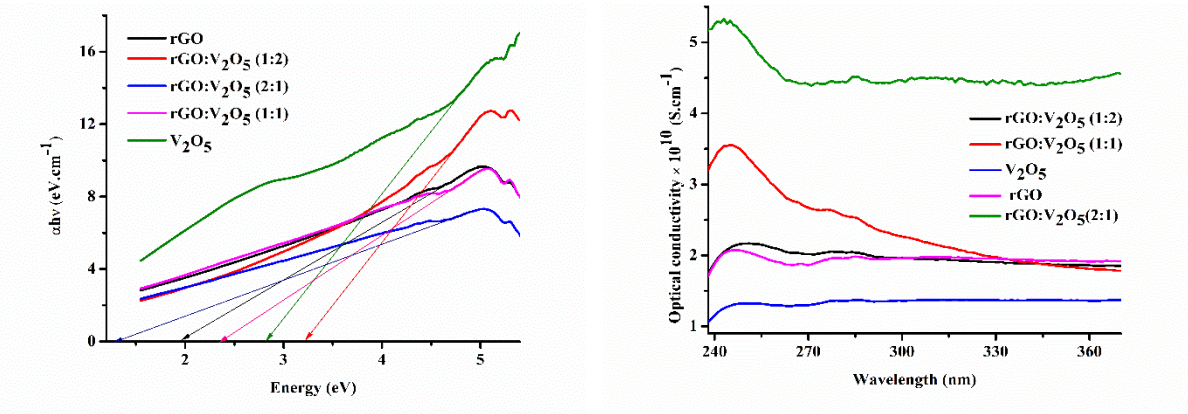

(a) **(b)**

Figure 2. (a) Band gap of rGO, V_2O_5, and synthesized composites; **(b)** Optical conductivity of rGO, V_2O_5, and synthesized composites.

3.2. Fourier transforms infrared (FTIR) spectroscopy.

The Fourier transform infrared spectra were observed with the help of KBr pellets using a Perkin Elmer spectrometer with a Diamond ATR detector ranging from around 400 to 4000 cm^{-1} with a resolution of 1 cm^{-1}.

3.2.1. FTIR of GO.

The FTIR spectra of GO (Figure 3) show the peaks 1063 cm^{-1}, which refers to the C-O stretching. The peak observed at 1224.85cm^{-1} confirms the C-O-C bending. Peak near 3342.37 cm^{-1} refers to OH stretching vibrations of C-OH group and water content. Peak observed near 1700 cm^{-1} shows the C=O stretch, and peaks near 1623 cm^{-1} show the C=C stretch [25].

3.2.2. FTIR of rGO.

In the IR spectra of rGO (as shown in Figure 3), the peaks observed in the GO, 1224, 3342, 1623, and 1700cm^{-1} are either removed or decreased, displaying that GO has been reduced to rGO. A peak near 1066cm^{-1} shows the presence of a C-O stretch in the compound. The peak near 1600 shows the presence of a C=C bond [26].

3.2.3. FTIR of V_2O_5.

In the IR spectra of V_2O_5 (as shown in Figure 3), the peak is observed near 1003, 830.23, 513.35, and 464cm^{-1}. Peaks observed near 1003cm^{-1} represent stretching vibrations for terminal bonds of oxygen (V=O). Peaks near 513.35cm^{-1} and 464cm^{-1} represent symmetric and asymmetric stretches of triply coordinated oxygens. Peaks observed near 830.23cm^{-1} represent vibrations of bridged oxygen [27].

3.2.4. FTIR of rGO: V_2O_5.

The peaks observed in Figure 3, near 3318cm^{-1} and 1699cm^{-1}, represent the O-H stretching and CO stretching, respectively. The peak observed near 1560cm^{-1} represents C=C stretching. The peaks observed near 1003cm^{-1} show stretching vibrations for terminal bonds of oxygen (V=O). Since rGO:V_2O_5 composite has peaks similar to both rGO and V_2O_5, It contributes to the characterization of the formation of the required composite [26-27].

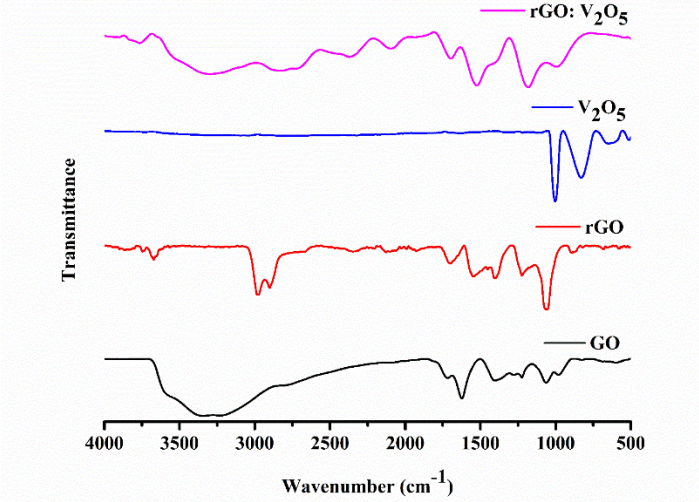

Figure 3. FTIR spectra of all the materials.

3.3. X-ray diffraction analysis.

X-ray diffraction (XRD) is a great analytical technique that helps predict a compound's material properties. The XRD machine used to characterize the samples is Bruker AXS D8 Advance A25-X1-1A2Z2C4B0. The spectra are recorded at a 2θ range of 10° - 70°, with the help of an anode copper source of Cu-Kα radiation (λ=1.54 Å) at the temperature of 25°C. In Fig. 4, a sharp peak was observed at 2θ =10.5°, and a weak peak near 21° suggests the formation of GO. The peak near 2θ =10° is disappeared in rGO due to the reduction process. The peak observed near 23° and 43° shows the reduction of GO to rGO. Since it is a broad peak, it is signified that crystallization has not occurred properly, and the compounds are amorphous. In Fig. 4, the peaks observed at 15.9°, 20.2°, 22.03°, and 31.1° refer to the orthorhombic phase of V_2O_5. Since the peaks observed are sharp, it suggests the presence of the crystalline nature of V_2O_5 [28]. In Fig. 4, the peaks were observed near 23° and 43°. Due to the interaction between V_2O_5 and rGO, the peaks present in rGO are intensified [29].

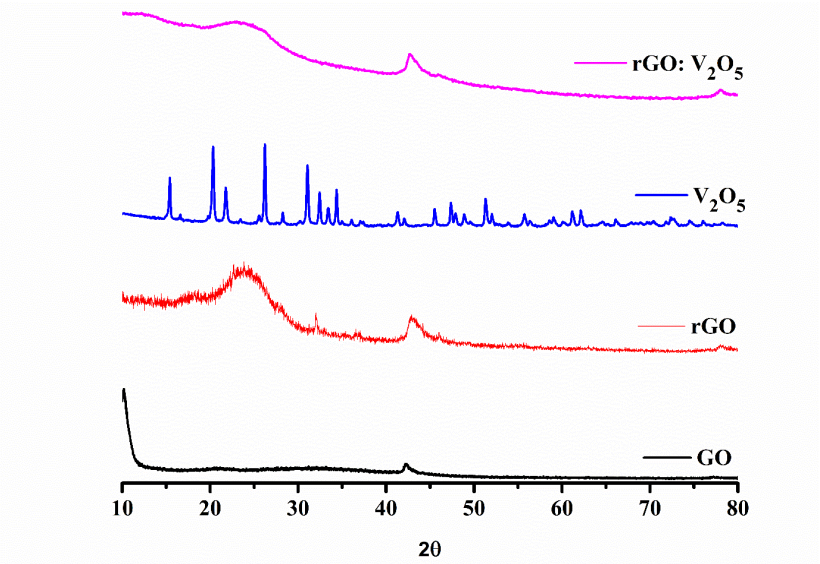

Figure 4. X-ray diffraction pattern for all the materials.

3.4. Scanning electron microscopy (SEM).

Scanning electron microscopy (SEM) is a technique used to study the morphology of compounds. The study of composite morphology is done using FE-SEM instrument model FESEM: JSM-7610F-Plus, Au Sputter Coater: DII-29030SCRT. Samples are coated with gold before the analysis. The scanning electron microscopy image of rGO: V_2O_5 composite is represented in Figure 5. The flake-like structures present in the FE-SEM images represent rGO. V_2O_5 particles present on the surface of rGO are observed to be agglomerated with each other, forming a bead-like structure [30].

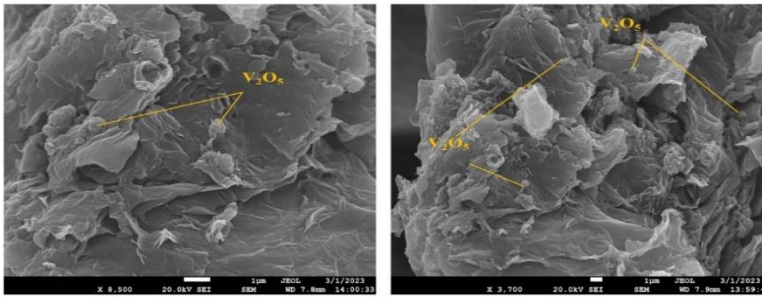

a)

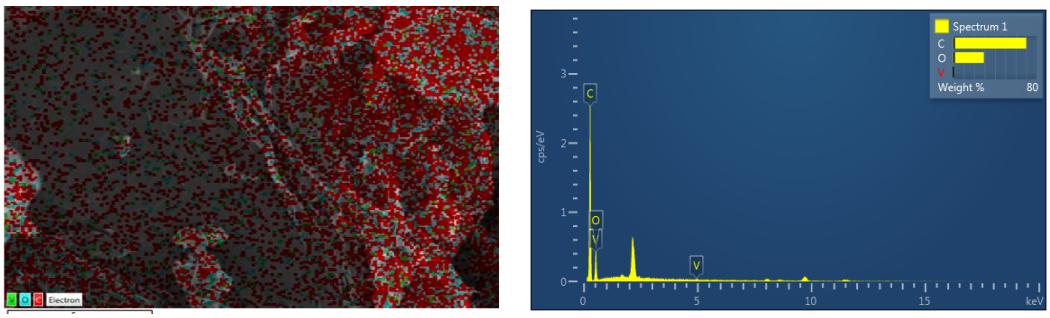

Figure 5. (a) Images of scanning electron microscopy of rGO: V_2O_5 (2:1) indicating the presence of V_2O_5 in the matrix of rGO; **(b)** EDS Layered image of FESEM rGO: V_2O_5 (2:1) representing the presence of expected elements; **(c)** Energy dispersive X-ray spectra of rGO: V_2O_5 (2:1).

3.5. Thermogravimetric analysis (TGA).

Thermogravimetric analysis (TGA) is an analysis technique used to measure the thermal stability of a compound. For the current studies, the instrument used is the Perkin Elmer thermal analyzer. The temperature range is between 75-580°C in nitrogen flow at a heating rate of 10ºC per minute. Figure. 6 represents the TGA curve of V_2O_5, rGO, and rGO: V_2O_5 (2:1) composite. In rGO, 16.25% weight loss was observed till 200°C. 200-400°C contributes to a weight loss of 37.09%, which is further lost to 44.58% till 515°C. V_2O_5 reduces 18% of its weight to 200°C, 37.5% to 400°C, and 46% to 515°C. In the case of composite rGO: V_2O_5, weight loss is 0.2% to 200°C, 0.7% to 400°C, and 1.05% to 515°C [27, 31].

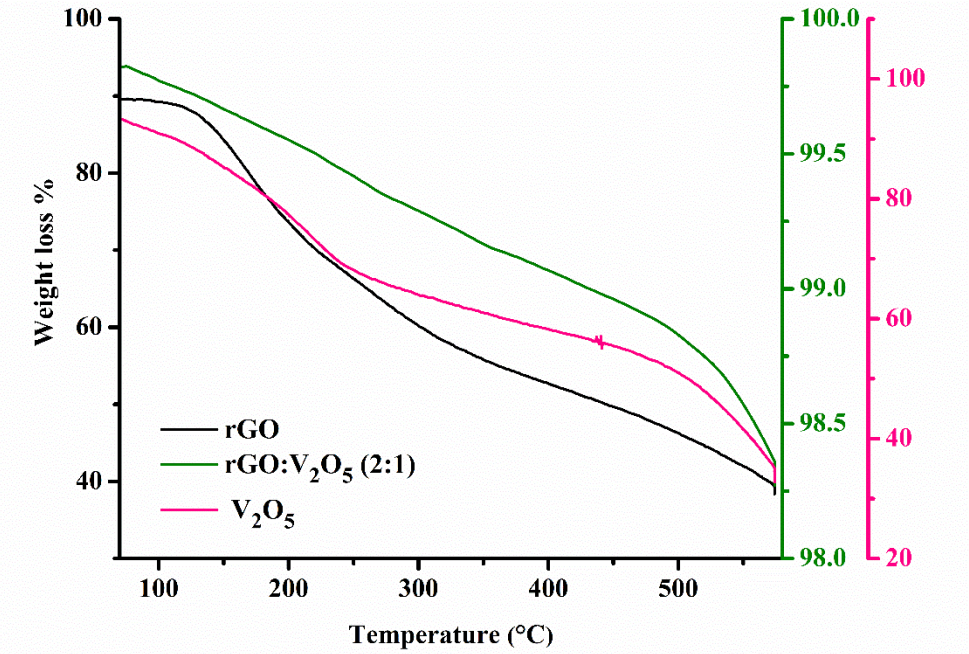

Figure 6. Thermogravimetric analysis of rGO, rGO:V2O5, V_2O_5.

4. Conclusions

Based on the current studies on optical band gap and optical conductivity of *ex-situ* fabricated rGO: V_2O_5, a great reduction in band gap is observed. This reduction is attributed to the introducing of defects in the rGO: V_2O_5 composites. rGO itself is a good material because it has less band gap. When it is combined with V_2O_5, an increase in carrier concentration and mobility is observed. Due to the reduction in band gap (1.32 eV) and increase in optical conductivity (5.34×10^{10} $S.cm^{-1}$) for rGO: V_2O_5 (2:1), the composites can be used for applications like solar cells and photodetectors.

Funding

No external funding was received to perform the above research work.

Acknowledgments

Presented in 4th International Conference on “Recent Advances in Fundamental and Applied Sciences” (RAFAS-2023)” on March 24-25, 2023, Organized by the School of Chemical Engineering and Physical Sciences, Lovely Professional University, Punjab, India.

Conflicts of Interest

The authors declare no financial or personal conflict of interest influences the work reported in this paper.

References

1. Kataria, S.; Rain, K.; Kumar, A.; Mudila H. Preparation and exploration of optical performance of novel polythiophene-ZrO2 composites. *Opt. Quant. Electron.* **2023,** *56*, 1-19, https://doi.org/10.1007/s11082-023-06046-3
2. Aawani, E.; Memarian, N.; Dizaji H.R. Synthesis and characterization of reduced graphene oxide–V_2O_5 nanocomposite for enhanced photocatalytic activity under different types of irradiation. *J. Phys. Chem. Solids* **2019**, *125*, 8-15, http://doi.org/10.1016/j.jpcs.2018.09.028.
3. Rikhari, R.; Saklani, B.; Bisht, A.; Mehtab, S.; Zaidi, M.; Haider, G. Graphene Oxide Assisted Modification in Electrical and Electrochemical Characteristics of Polypyrrole. *Sens. Lett*. **2019**, *17*, 511-515, https://doi.org/10.1166/sl.2019.4116.
4. Kambhala, N.; Kaveramma, A.B.; Angappane, S.; Shwetha, R.R.;Thiyagaraj, S.; Akkera, H.S. Effects of the phase, morphology, band gap and hydrogen evolution of vanadium oxide with reduced graphene oxide. *Mater. Today Commun*. **2023**, *34*, 105478, https://doi.org/10.1016/j.mtcomm.2023.105478.
5. Ahmed, A.; Singh, A.; Young, S.-J.; Gupta, V.; Singh, M.; Arya, S. Synthesis techniques and advances in sensing applications of reduced graphene oxide (rGO) Composites: A review. *Compos. Part A Appl. Sci. Manuf.* **2023**, *165*, 107373, https://doi.org/10.1016/j.compositesa.2022.107373.
6. Politano, G.G.; Versace, C. Electrical and Optical Characterization of Graphene Oxide and Reduced Graphene Oxide Thin Films. *Crystals* **2022**, *12*, 1312, https://doi.org/10.3390/cryst12091312.
7. Razaq, A.; Bibi, F.; Zheng, X.; Papadakis, R.; Jafri, S.H.M.; Li, H. Review on Graphene-, Graphene Oxide-, Reduced Graphene Oxide-Based Flexible Composites: From Fabrication to Applications. *Materials* **2022**, *15*, 1012, https://doi.org/10.3390/ma15031012.
8. Eivazzadeh-Keihan, R.; Noruzi, E.B.; Chidar, E.; Jafari, M.; Davoodi, F.; Kashtiaray, A.; Gorab, M.G.; Hashemi, S.M.; Javanshir, S.; Cohan, R.A.; Maleki, A.; Mahdavi, M. Applications of carbon-based conductive nanomaterials in biosensors. *Chem. Eng. J.* **2022**, *442*, 136183, https://doi.org/10.1016/j.cej.2022.136183.
9. Yadav, A.A.; Hunge, Y.M.; Kang, S.-W.; Fujishima, A.; Terashima, C. Enhanced Photocatalytic Degradation Activity Using the V_2O_5/RGO Composite. *Nanomaterials* **2023**, *13*, 338, https://doi.org/10.3390/nano13020338.
10. Alsafari, I.A.; Chaudhary, K.; Warsi, M.F.; Warsi, A.-Z.; Waqas, M.; Hasan, M.; Jamil, A.; Shahid, M. A facile strategy to fabricate ternary WO_3/CuO/rGO nano-composite for the enhanced photocatalytic degradation of multiple organic pollutants and antimicrobial activity. *J. Alloys Comp*. **2023**, *938*, 168537, https://doi.org/10.1016/j.jallcom.2022.168537.
11. Kataria, S.; Mudila, H.; Kumar, A.; Prasher, P. Optical Properties of Novel Materials for Optoelectronic Applications. *Nanosci. Nanotechnol. -Asia* **2022**, *12*, 48-57, http://doi.org/10.2174/2210681213666221031103157.
12. Samiei, E.; Mohammadi, S.; Torkzadeh-Mahani, M. Effect of gamma-irradiation on electrochemical properties of $ZnCo_2O_4$-rGO for supercapacitor application. *Diam. Relat. Mater.* **2022**, *127*, 109157, https://doi.org/10.1016/j.diamond.2022.109157.
13. Papaj, M.; Moore, J.E. Current- enabled optical conductivity of superconductors. *Phys.Rev. B* **2022**, *106*, L220504, https://doi.org/10.1103/PhysRevB.106.L220504.

14. Guerrero-Contreras, J.; Caballero-Briones F. Graphene oxide powders with different oxidation degree, prepared by synthesis variations of the Hummers method. *Mater. Chem. Phy.* **2015**, *153*, 209-220, https://doi.org/10.1016/j.matchemphys.2015.01.005.
15. Méndez-Lozano, N.; Pérez-Reynoso, F.; González-Gutiérrez, C. Eco-Friendly Approach for Graphene Oxide Synthesis by Modified Hummers Method. *Materials* **2022**, *15*, 7228, https://doi.org/10.3390/ma15207228.
16. Habte, A.T.; Ayele, D.W. Synthesis and Characterization of Reduced Graphene Oxide (rGO) Started from Graphene Oxide (GO) Using the Tour Method with Different Parameters. *Adv. Mater. Sci. Eng.* **2019**, *2019*, 5058163, https://doi.org/10.1155/2019/5058163.
17. Korucu, H. Evaluation of the performance on reduced graphene oxide synthesized using ascorbic acid and sodium borohydride: Experimental designs-based multi-response optimization application. *J. Mol. Struct.* **2022**, *1268*, 133715, https://doi.org/10.1016/j.molstruc.2022.133715.
18. Chen, D.; Yi, R.; Chen, S.; Xu, T.; Gordin, M.L.; Lv, D.; Wang, D. Solvothermal synthesis of V_2O_5/graphene nanocomposites for high performance lithium ion batteries. *Mater. Sci. Eng. B* **2014**, *185*, 7-12, https://doi.org/10.1016/j.mseb.2014.01.015.
19. Sunderrajan, S.; Miranda, L.R.; Pennathur, G. Improved stability and catalytic activity of graphene oxide/chitosan hybrid beads loaded with porcine liver esterase. *Prep. Biochem. Biotechnol.* **2018**, *48*, 343-351, https://doi.org/10.1080/10826068.2018.1446153.
20. Rabchinskii, M.K. ; Shnitov, V.V.; Dideikin, A.T.; Aleksenskii, A.E.; Vul, S.P.; Baidakova, M.V.; Pronin, I.I.; Kirilenko, D.A.; Brunkov, P.N.; Weise, J.; Molodtsov, S.L. Nanoscale Perforation of Graphene Oxide during Photoreduction Process in the Argon Atmosphere *J. Phys. Chem. C* **2016**, *120*, 28261–28269, https://doi.org/10.1021/acs.jpcc.6b08758.
21. Handayani, M.; Suwaji, B.I.; Ihsantia Ning Asih, G.; Kusumaningsih, T.; Kusumastuti, Y.; Rochmadi; Anshori, I. In-situ synthesis of reduced graphene oxide/silver nanoparticles (rGO/AgNPs) nanocomposites for high loading capacity of acetylsalicylic acid. *Nanocomposites* **2022**, *8*, 74-80, https://doi.org/10.1080/20550324.2022.2054210.
22. Shen, Y.; Yang, S.; Zhou, P.; Sun, Q.; Wang, P.; Wan, L.; Li, J.; Chen, L.; Wang, X.; Ding, S.; Zhang, D.W. Evolution of the band-gap and optical properties of graphene oxide with controllable reduction level. *Carbon* **2013**, *62*, 157-164, https://doi.org/10.1016/j.carbon.2013.06.007.
23. McGhee, J.; Georgiev, V.P. Simulation Study of Surface Transfer Doping of Hydrogenated Diamond by MoO_3 and V_2O_5 Metal Oxides. *Micromachines* **2020**, *11*, 433, https://doi.org/10.3390/mi11040433.
24. Mondal, S.; Sen, S.; Kumar, A.; Mudila, H. Modulation of optical band gap and conductivity of polyindoles with concentrations of $FeCl_3$ and APS. *Results Opt.* **2023**, *13*, 1-11, https://doi.org/10.1016/j.rio.2023.100556
25. Sudesh; Kumar, N.; Das, S.; Bernhard, C.; Varma, G.D. Effect of graphene oxide doping on superconducting properties of bulk MgB_2. *Supercond. Sci. Technol.* **2013**, *26*, 095008, https://doi.org/10.1088/0953-2048/26/9/095008.
26. Singhal, K.; Mehtab, S.; Pandey, M.; Zaidi, M.G.H. Sustainable development of graphene oxide from pine leaves for electrochemical energy storage and corrosion protection. *Curr. Res. Green Sustain Chem*. **2022**, *5*, 100266, https://doi.org/10.1016/j.crgsc.2022.100266.
27. Xavier, J.R. High protection performance of vanadium pentoxide-embedded polyfuran/epoxy coatings on mild steel. *Polym. Bull.* **2021**, *78*, 5713-5739, https://doi.org/10.1007/s00289-020-03400-3.
28. Prasad, K.S.; Shivamallu, C.; Shruthi, G.; Prasad, M. A Novel and One-pot Green Synthesis of Vanadium Oxide Nanorods Using a Phytomolecule Isolated from *Phyllanthus amarus*. *Chem. Select* **2018**, *3*, 3860-3865, https://doi.org/10.1002/slct.201800653.
29. Bhardwaj, D.; Sangwan, S.; Shivashankar, S.A.; Umarji, A.M. Microwave-assisted synthesis of reduced graphene oxide/V2O5 nano-composite as an efficient photocatalyst for dye degradation. *Bull. Mater. Sci.* **2022**, *45*, 135, https://doi.org/10.1007/s12034-022-02707-3.
30. Palanisamy, K.; Um, J.H. , Jeong, M.; Yoon, W.-S. Porous V_2O_5/RGO/CNT hierarchical architecture as a cathode material: Emphasis on the contribution of surface lithium storage. *Sci. Rep.* **2016**, *6*, 31275, https://doi.org/10.1038/srep31275.
31. Tene, T.; Tubon Usca, G.; Guevara, M.; Molina, R.; Veltri, F.; Arias, M.; Caputi, L.S.; Vacacela Gomez, C. Toward Large-Scale Production of Oxidized Graphene. *Nanomaterials* **2020**, *10*, 279, https://doi.org/10.3390/nano10020279.